

Influence of Main Chain on the Phase Behaviors of Side-Chain Liquid-Crystalline Polymers with Triphenylene Mesogens of Long Alkyl Tail Substituents

Ping Li,¹ Sheng Chen,¹ Hang Luo,² Dou Zhang,² Hailiang Zhang¹

¹Key Laboratory of Polymeric Materials and Application Technology of Hunan Province, Key Laboratory of Advanced Functional Polymer Materials of Colleges and Universities of Hunan Province, College of Chemistry, Xiangtan University, Xiangtan, Hunan Province 411105, China

²State Key Laboratory of Powder Metallurgy, Central South University, Changsha, Hunan 410083, China

Correspondence to: S. Chen (E-mail: huaxuechensheng@163.com) or H. Luo (E-mail: xtluoang@163.com) or H. Zhang (E-mail: zh11965@xtu.edu.cn)

Received 8 July 2016; accepted 8 November 2016; published online 00 Month 2016

DOI: 10.1002/pola.28428

ABSTRACT: A series of side-chain liquid-crystalline polymers (SCLCPs) containing triphenylene mesogen, in which the long alkyl tail Tp connected directly with main chain, were synthesized successfully. The chemical structures of the monomers were confirmed by ¹H NMR and mass spectrometry. The phase behaviors of polymers were investigated by a combination of techniques, including DSC, POM, 1D/2D WAXD, and SAXS. The experimental results suggested that the type of main chain played an important role in the LC phase structures of these polymers. Because of the steric effects of side chains and the coupling effects between the Tp moieties and the main chains, all the polymers exhibited columnar phase. However, the

SCLCPs with poly(vinyl benzene methyl ether) or polynorbornene backbone displayed hexagonal columnar phase, while those with polyacrylate or polymethacrylate backbone presented columnar nematic phase, and the one with poly(vinyl benzoate) main chain showed rectangular columnar phase. Moreover, the clearing temperatures (Ti) changed with change in main chain. Especially, the Ti of the SCLCP with polymethacrylate backbone was above 300 °C. © 2016 Wiley Periodicals, Inc. *J. Polym. Sci., Part A: Polym. Chem.* **2016**, *00*, 000–000

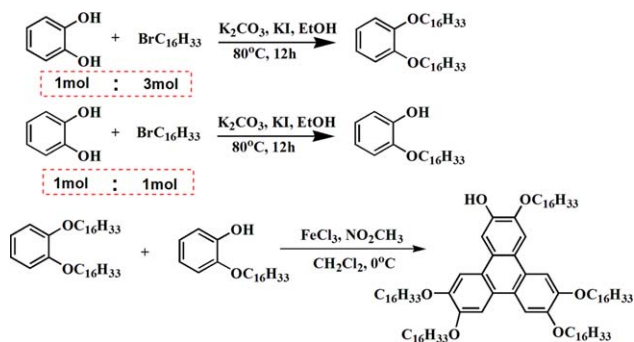
KEYWORDS: main chain; phase behavior; structure-property relations; liquid-crystalline polymers; triphenylene mesogen

INTRODUCTION Side-chain liquid-crystalline polymers (SCLCPs), due to the combination of properties of both, liquid crystals and polymers, possess good processability, film-formation ability, and good mechanical properties and hence, have attracted great attention.^{1–5} Due to the π - π stacking of the planar aromatic cores and the interactions of the peripheral chains, discotic SCLCPs (DSCLCPs) can self-assemble into well-ordered supramolecular structures, which find applications as organic superconducting materials or organic magnetic materials.^{6–8} For example, the triphenylene (Tp)-based SCLCPs have been widely investigated because they possess several advantages, such as relatively easy synthesis, thermal and chemical stability, excellent charge carrier mobility, and varieties of mesophases.^{9–11} Recently, a comparative study was conducted to investigate the effect of molecular weight on phase structure, specifically to gain a deeper insight of the influence of spacer length of DSCLCPs, based on a homologous series of well-defined discotic liquid-crystalline polyacrylates with Tp side groups with different spacer lengths by Chen et al.^{12,13}

Tp-based SCLCPs are comprised of four distinct structural units: the main chain, the spacer, the Tp discotic mesogenic

group, and the tail.^{14–21} By making changes in the chemical structure, the phase transitions and phase structures of Tp-based SCLCPs can be tailored accordingly, which make them useful for organic electronics and optoelectronic applications.^{22,23} For example, Zeng et al. studied the self-organization behaviors of pendant mesogenic Tp-based SCLCPs with regioregular polythiophene backbone and different spacer lengths.²⁴ The results showed that polymers could self-organize into mesophases possessing intertwined lamello-columnar morphologies, though to different extents. This was a result of the simultaneous coexistence of lamellar and columnar sublattices. Xing et al. investigated the influence of different alkyl chain lengths of liquid-crystalline polymers with triphenylene-containing 1-decyne on mesomorphic properties.²⁵ The results showed that the polymers with shorter and longer alkyl chain lengths adopted a homogeneous hexagonal columnar structure, whereas those with intermediate lengths formed mesophases with mixed structures. Later, Yu et al. investigated the mesomorphic properties and phase behaviors of novel SCLCPs with triphenylene-containing acetylenes, having one or three methylene units as the spacer.²⁶ The polymers

© 2016 Wiley Periodicals, Inc.



SCHEME 1 Synthetic route for the synthesis of 2-hydroxy-3,6,7,10,11-pentakis(hexadecyloxy)triphenylene. [Color figure can be viewed at wileyonlinelibrary.com]

adopted a columnar shape and self-organized into a hexagonally packed columnar phase. Zhu et al. discussed the LC behaviors of mesogen-jacketed liquid-crystalline polymers, containing two Tp units, with different number of methylene units between the terephthalate core and Tp moieties in the side chains.^{27,28} With increase in spacer length and temperature, the polymers exhibited interesting phase behaviors. Recently, our group studied the effect of spacer length and alkyl tail length on the phase behaviors of Tp-based SCLCPs.^{29,30} By changing the spacer length and tail length, the phase behaviors and phase structures of Tp-based SCLCPs were studied elaborately. However, still there are only few reports that focus on the LC behavior of Tp-based SCLCPs with varying main chain and on the investigation of the phase structure. Study of the phase behaviors of the complete homologous series would help in designing of new polymers having tailored phase behavior in a rational manner.

Mesogen-jacketed liquid-crystalline polymers (MJLCPs), in which mesogenic units are laterally attached to the main chain through only one covalent C–C bond or a very short spacer, have gained tremendous interest. This is due to their novel structures and properties, such as high glass transition temperatures, broad temperature ranges of mesophase, formation of banded structures texture after mechanical shearing in LC state and an ideal rod-forming system.^{31–37} However, the synthesis of MJLCPs is very difficult. It is well known that these properties of MJLCPs are a result of the strong coupling and steric effects. Based on those two points, it can be conceptualized that Tp containing the long alkyl tail SCLCPs, without the spacer or short spacer, can produce the “jacketing effect.”^{38–40} On one hand, it is easy to synthesize Tp-based SCLCPs without the spacer or short spacer. On the other hand, Tp with long alkyl tails has a large steric volume and there is also a strong coupling effect between the main chain and Tp mesogen.

In this work, a series of long alkyl tail Tp-based SCLCPs, containing either short spacer or no spacer, with variation in main chain, has been synthesized. The chemical structures of the polymers are shown in Scheme 1. The main chain of Tp-based SCLCPs is either polyacrylate, polymethacrylate,

poly(vinyl benzoate), poly(vinyl benzene methyl ether), or polynorbornene. For convenience, the corresponding polymers were designated as PMTP, PMMTP, PSTP, POTP, and PNVTP, respectively. Phase behaviors of the polymers were studied by DSC, POM, 1D/2D XRD, and SAXS. The experimental results showed that the nature of main chain plays an important role in the LC phase structures of these polymers. POTP and PNVTP exhibited the hexagonal columnar (Φ_H) phase. PMMTP and PMTP showed the nematic columnar (Φ_N) phase, whereas PSTP showed the rectangular columnar (Φ_R) phase. In addition, all the polymers exhibited only weak π – π interactions of the side-chain triphenylene mesogens, due to the strong coupling effects between the main chains with the triphenylene mesogen.

EXPERIMENTAL

Materials

Anhydrous tetrahydrofuran (THF) was distilled from sodium benzophenone ketyl under argon atmosphere and used immediately. Triethylamine (TEA) and dichloromethane (CH₂Cl₂) were dried over anhydrous magnesium sulfate. Chlorobenzene (Acros 99%) was purified by washing with concentrated sulfuric acid to remove residual thiophenes, followed by washing, first with 5% sodium carbonate solution, and then with water before it was dried over anhydrous calcium chloride and distilled. 2,2-Azobisisobutyronitrile (AIBN) was freshly recrystallized from methanol. Pyrocatechol (98%, Alfa Aesar) and bromoalkanes along with other reagents and solvents were used as received without further purification.

Synthesis of Monomers

The chemical structures and synthetic procedures of five monomers are shown in Scheme 1. 2-Hydroxy-3,6,7,10,11-pentakis(hexadecyloxy)triphenylene was synthesized successfully according to the literature procedure.²⁵ Detailed procedures for the synthesis of the other monomers are as follows:

2-Hexadecyloxyphenol and 1,2-Di(hexadecyloxy) Benzene

2-Hexadecyloxyphenol and 1,2-di(hexadecyloxy)benzene were conveniently synthesized using different molar ratios. For the synthesis of 1,2-di(hexadecyloxy)benzene, 1,2-dihydroxybenzene (10 g, 0.091 mol), 1-bromohexadecane (83 g, 0.274 mol), K₂CO₃ (36 g, 0.26 mol), a little bit of KI and ethanol (500 mL) were taken in 1-L round-bottom flask and the reaction mixture was refluxed for 12 h. After this, the reaction mixture was poured into ice water (5 L). The crude solid product obtained was collected by filtration and dried under vacuum. It was then purified using column chromatography using silica gel.

2-Hexadecyloxyphenol was prepared using the same procedure, except for the following changes: 1,2-dihydroxybenzene (10 g, 0.091 mol), 1-bromohexadecane (27.5 g, 0.091 mol), K₂CO₃ (36 g, 0.26 mol), a little bit of KI and ethanol (500 mL) were taken in 1-L round-bottom flask and the reaction mixture was refluxed for 12 h. After this, the reaction mixture was poured into ice water (5 L). The crude solid product obtained

was collected by filtration and dried under vacuum. It was then purified using column chromatography using silica gel

2-Hydroxy-3,6,7,10,11-Pentakis(Hexadecyloxy) Triphenylene

In a 1-L round-bottom flask, placed in an ice-water bath, were dissolved 1,2-di(hexadecyloxy)benzene (20 g, 0.036 mol), 2-hexadecyloxyphenol (6 g, 0.018 mol), and nitromethane (30 mL) in dried CH₂Cl₂ (500 mL). Then FeCl₃ (35 g, 0.21 mol) was added to the above solution, under vigorous stirring. After 3 h, the solution was further stirred at room temperature for 1 h. Cold methanol (100 mL) was then slowly added to the reaction mixture. The organic phase was washed with water three times and dried over anhydrous MgSO₄. After removal of the solvent, the crude product was purified by silica-gel column chromatography. (MS) (*m/z*) Calcd. for C₉₈H₁₇₂O₆, 1445.32; found, 1445.383.

[3,6,7,10,11-Pentakis(hexadecyloxy)-2-oxytriphenylene] Methacrylate

HO-R (0.8 g, 0.00055 mol) and TEA (3 mL) were dissolved in dry THF (50 mL) to obtain solution A. In another flask, methacryloyl chloride (0.84 g, 0.0081 mol) was dissolved in dry THF (20 mL) to obtain solution B. The flask containing solution A was cooled in an ice-water bath, and solution B was slowly added to the solution A, over a period of 0.5 h. The resultant mixture was further stirred at room temperature for 10 h. Most of the THF was distilled off under reduced pressure. This was followed by addition of water to the residue. The crude solid product was first collected by filtration and dried under vacuum. The product was purified by column chromatography on silica gel, using dichloromethane as the eluent.

¹H NMR (400 MHz, CDCl₃, ppm): 8.22–8.17 (1H, Ar-H), 7.88–7.74 (a, 1H, Ar-H, b, 1H, Ar-H, c and d, 1H, Ar-H, e, 1H, Ar-H, f, 1H, Ar-H), 6.75 (m, 1H, =CH₂), 6.56 (l, 1H, -CH=), 6.04 (n, 1H, =CH₂), 4.24–4.19 (g, 10H, -CH₂-), 1.97–1.82 (h, 10H, -CH₂-), 1.51–1.44 (j, 10H, -CH₂-), 1.33–1.25 (i, 120H, -CH₂-), 1.36–1.26 (k, 10H, -CH₂-), 0.95–0.92 (l, 15H, -CH₃). (MS) (*m/z*) [M] Calcd for C₁₀₁H₁₇₄O₇, 1500.33; found, 1499.609.

[3,6,7,10,11-Pentakis(hexadecyloxy)-2-oxytriphenylene]methyl Methacrylate

The [3,6,7,10,11-Pentakis(hexadecyloxy)-2-oxytriphenylene]-methyl methacrylate (MMTP) monomer was synthesized by a procedure very similar to MTP, mentioned earlier. ¹H NMR (400 MHz, CDCl₃, ppm): 8.22–8.17 (b, 1H, Ar-H, c, 1H, Ar-H), 7.88–7.74 (a, 1H, Ar-H, d, 1H, Ar-H, e, 1H, Ar-H, f, 1H, Ar-H), 6.45 (o, 1H, =CH₂), 5.81 (n, 1H, =CH₂), 4.24–4.19 (g, 10H, -CH₂-), 2.14 (m, 3H, =C-CH₃), 1.97–1.82 (h, 10H, -CH₂-), 1.51–1.44 (j, 10H, -CH₂-), 1.33–1.25 (i, 120H, -CH₂-), 1.36–1.26 (k, 10H, -CH₂-), 0.95–0.92 (l, 15H, -CH₃). MS (*m/z*) Calcd. for C₁₀₂H₁₇₆O₇, 1514.34; found, 1513.775.

N-4-[3,6,7,10,11pentakis(Hexadecyloxy)-2-Oxytriphenylene]Benzoate}-Cis-5-Norbomene-Exo-2,3-Dicarboximide (NVTP)

N-4-benzoate-cis-5-norbomene-exo-2,3-dicarboximide was synthesized according to a reported procedure.⁴¹ N-4-benzoate-cis-5-norbomene-exo-2,3-dicarboximide (1.0 g) and HO-R (1.0 g,

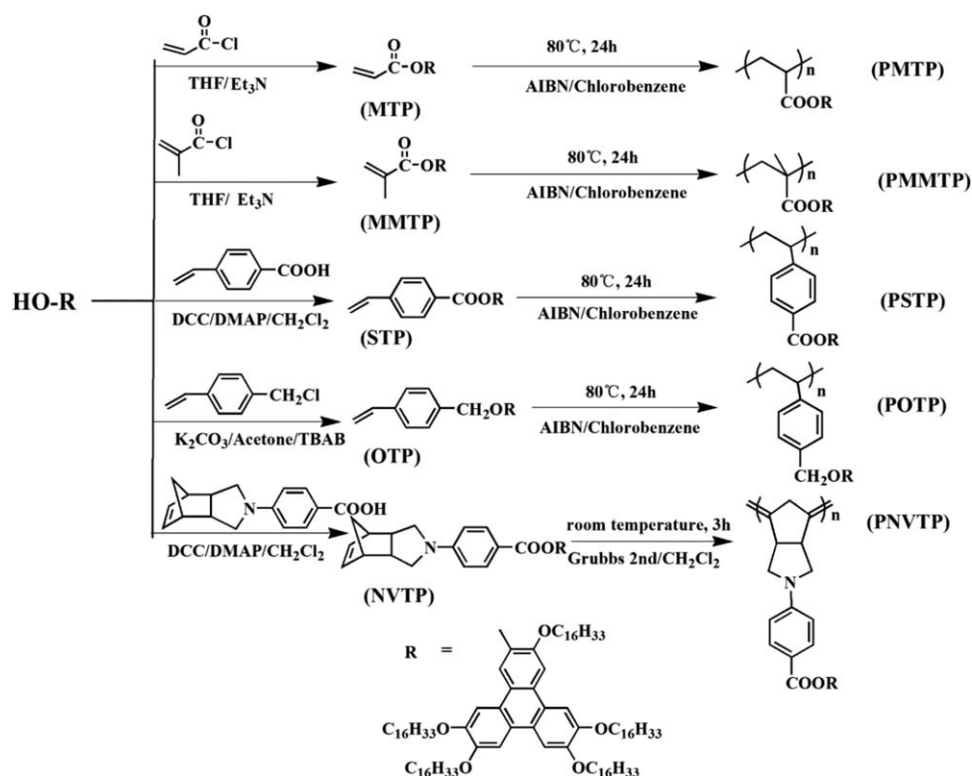
0.69 mmol) were dissolved in dry CH₂Cl₂ (100 mL) at room temperature. N, N'-dicyclohexylcarbodiimide (DCC, 1.2 g, 5.8 mmol) and 4-dimethylaminopyridine (0.5 g, 1.8 mmol) were added to the solution. The mixture was then stirred at room temperature for 10 h. After this the reaction mixture was diluted with CH₂Cl₂ (200 mL). The resulting solution was washed with water (100 mL) three times. The organic phase was dried over anhydrous MgSO₄, filtered and the solvent was removed. The crude product was purified by column chromatography using silica gel with dichloromethane as eluent. ¹H NMR (400 MHz, CDCl₃, ppm): 8.49–8.11 (b, 1H, Ar-H, c, 1H, Ar-H, f, 1H, Ar-H), 7.98–7.61 (d, 1H, Ar-H, l, 1H, Ar-H), 6.96 (e, 1H, Ar-H), 6.47 (m, 1H, Ar-H), 5.00 (q, 2H, -HC = CH-), 4.30 (g, 10H, -CH₂-), 3.41 (n, 2H, -CH-), 2.97 (o, 2H, -CH-), 2.25 (p, 2H, -CH₂-), 1.97–1.82 (h, 10H, -CH₂-), 1.51–1.44 (j, 10H, -CH₂-), 1.33–1.25 (i, 120H, -CH₂-), 1.36–1.26 (k, 10H, -CH₂-), 0.95–0.92 (l, 15H, -CH₃). (MS) (*m/z*) [M] Calcd for C₁₁₃H₁₈O₇N, 1711.39; found, 1710.547.

4-[3,6,7,10,11-Pentakis(Hexadecyloxy)-2-Oxymethylenetriphenylene]Styrene (OTP)

Vinylbenzyl chloride (1.2 g, 7.84 mmol), K₂CO₃ (0.6 g, 4.3 mmol) and very little of tetrabutylammonium bromide (TBAB, 80 mg, 0.25 mmol) were dissolved in acetone (100 mL). Then HO-R (0.8 g) and a drop of nitrobenzene were added. The reaction mixture was stirred under reflux and nitrogen atmosphere for 12 h in an oil bath. After this, the reaction mixture was poured into a large amount of water. The crude product obtained was dried and then purified by column chromatography, using dichloromethane as the eluent. ¹H NMR (400 MHz, CDCl₃, ppm): 7.99–7.74.17 (b, 1H, Ar-H, c, 1H), 7.68–7.39 (a, 1H, Ar-H, d, 1H, Ar-H, e, 1H, Ar-H, f, 1H, Ar-H, m, 1H, Ar-H, n, 1H, Ar-H), 6.73 (o, 1H, Ar-CH=), 5.71 (p, 1H, =CH₂), 5.41 (l, 2H, -CH₂-), 5.28 (q, 1H, =CH₂), 4.24–4.19 (g, 10H, -CH₂-), 1.97–1.82 (h, 10H, -CH₂-), 1.51–1.44 (j, 10H, -CH₂-), 1.33–1.25 (i, 120H, -CH₂-), 1.36–1.26 (k, 10H, -CH₂-), 0.95–0.92 (l, 15H, -CH₃). MS (*m/z*) Calcd. for C₁₀₇H₁₀₈O₆, 1562.38; found, 1561.753.

[3,6,7,10,11-Pentakis(Hexadecyloxy)-2-Oxytriphenylene]Vinylbenzoate (STP)

N, N'-dicyclohexylcarbodiimide (DCC, 1.7 g, 8.4 mmol), 4-dimethylaminopyridine(DMAP, 50 mg, 0.04 mol), HO-R(1.2 g, 0.84 mmol), and 4-vinylbenzoic acid(1.2 g, 84 mmol) were dissolved in CH₂Cl₂ solution and stirred for 10 h at room temperature. Then the mixture was diluted with CH₂Cl₂ (200 mL). The organic phase was washed with water (100 mL) three times and the organic phase was dried over anhydrous MgSO₄, filtered and evaporated. The crude product was purified by column chromatography on silica gel, with dichloromethane as eluent. ¹H NMR (400 MHz, CDCl₃, ppm): 8.22–8.17 (b, 1H, Ar-H, c, 1H, Ar-H, f, 1H, Ar-H, l, 1H, Ar-H), 7.90–7.74 (a, 1H, Ar-H, e, 1H, Ar-H), 7.56 (m, 1H, Ar-H), 6.81 (n, 1H, Ar-CH=), 5.97 (p, 1H, =CH₂), 5.45 (o, 1H, =CH₂), 4.24–4.19 (g, 10H, -CH₂-), 1.97–1.82 (h, 10H, -CH₂-), 1.51–1.44 (j, 10H, -CH₂-), 1.33–1.25 (i, 120H, -CH₂-), 1.36–1.26 (k, 10H, -CH₂-), 0.95–0.92 (l, 15H, -CH₃). (MS) (*m/z*) [M] Calcd for C₁₀₇H₁₇₈O₇, 1574.36; found, 1576.050.



SCHEME 2 Routes for the synthesis of monomers and their corresponding polymers.

Polymerization

All the polymers, except PNVTP were synthesized by the conventional solution radical polymerization method (Scheme 2). The general procedure for the synthesis of all polymers, PMTP, PATP, POTP, and PSTP, by conventional solution radical polymerization is as follows:

Appropriate quantities of the monomer, AIBN, and THF were taken in a dry reaction tube containing a magnetic stirring bar. The molar ratio of monomer to AIBN, $N_{\text{monomer}}: N_{\text{AIBN}} = 100: 1$, and the monomer mass concentration was 50%. After three freeze-pump-thaw cycles, the tube was sealed under vacuum. Polymerization was carried out at 80°C for 24 h. The sample was purified by precipitation from THF thrice, followed by hot acetone. Lastly, the sample dried under vacuum.

PNVTP was synthesized by ring-open metathesis polymerization (ROMP). Details of the procedure are as follows:

NVTP (200 mg) and Grubb's second-generation catalyst (2.1 mg) were taken in a dry Schlenk tube along with a magnetic stirring bar. After three pump-purge cycles with high purity nitrogen, CH_2Cl_2 (~ 2 mL) was injected into the mixture and left to stir at room temperature for 3 h. A few drops of vinyl ethyl ether were added to the reaction mixture using a syringe. After an additional hour, the polymer solution was diluted with CH_2Cl_2 (5 mL). The obtained PNVTP was purified on a short alumina column and then the polymer was precipitated in methanol (100 mL). Lastly, the product was dried in a vacuum oven for 12 h.

Instruments and Measurements

^1H NMR spectroscopy was carried on a Bruker ARX400 MHz spectrometer using CDCl_3 as the solvent and tetramethylsilane (TMS) as the internal standard at ambient temperature. The chemical shifts were reported in ppm.

The apparent number average molecular weight (M_n) and polydispersity index ($\text{PDI} = M_w/M_n$) were determined by GPC (WATERS 1515 instrument) with a set of HT3, HT4 and HT5. The μ -styragel columns used THF as an eluent and the flow rate was 1.0 mL min^{-1} at 38°C . All the GPC data were calibrated by polystyrene standards.

TGA was performed on a TA SDT 2960 instrument at a heating rate of $20^\circ\text{C min}^{-1}$ in nitrogen atmosphere.

DSC traces of the polymer were obtained using a TA Q10 DSC instrument. The temperature and heat flow were calibrated using standard materials (indium and zinc) at cooling and heating rates of $10^\circ\text{C min}^{-1}$. Typically, a sample of mass of about 5 mg was sealed in aluminum pans.

LC texture of the polymers was examined using POM (Leica DM-LM-P), equipped with a Mettler Toledo hot stage (FP82HT).

One-dimensional wide-angle X-ray diffraction (1D WAXD) experiments were performed on a BRUKER AXS D8 Advance diffractometer, equipped with a 40-kV FL tube as the X-ray source ($\text{Cu K}\alpha$) and the LYNXEYE_XE detector. Background scattering was recorded and subtracted from the sample patterns. The heating and cooling rates in the 1D WAXD experiments were $10^\circ\text{C min}^{-1}$.

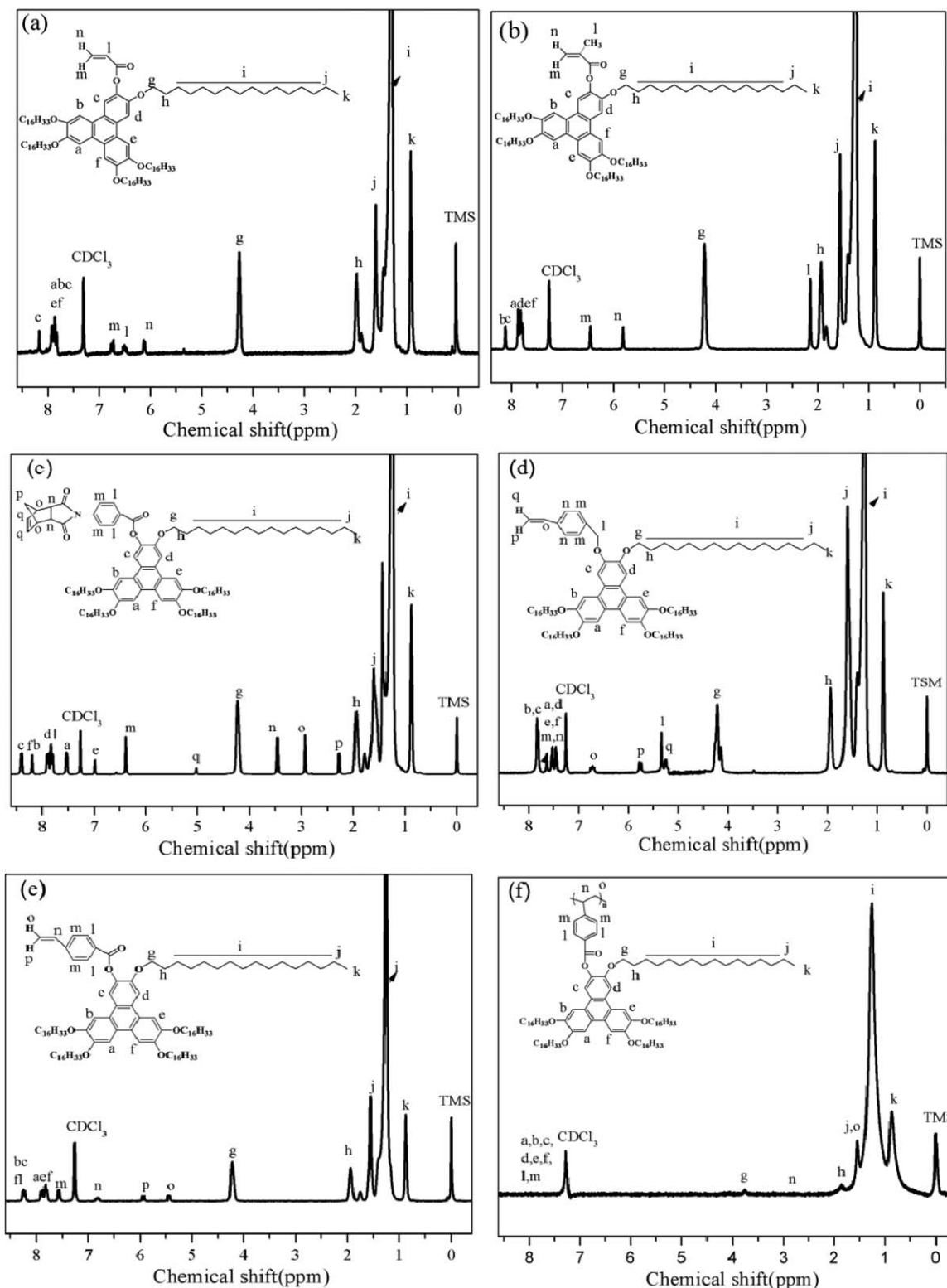


FIGURE 1 ^1H NMR spectra of monomers and the polymer PSTP.

Two-dimensional wide-angle X-ray diffraction (2D WAXD) was carried out using a BRUKER AXS D8 Discover diffractometer, equipped with a 40-kV FL tube as the X-ray source (Cu $K\alpha$) and VANTEC 500 detector. The point-focused X-ray

beam was aligned either perpendicular or parallel to the mechanical shearing direction. For both the 1D and 2D WAXD experiments, the background scattering was recorded and subtracted from the sample patterns.

TABLE 1 Molecular Characteristics and Properties of the Series of Polymers

Sample	M_n ($\times 10^{-4}$ g mol $^{-1}$) ^a	PDI ^a	T_d (°C) ^b	T_g (°C) ^c	T_i (°C) ^d	LC ^e	T_m (°C) ^c
PMMTP	49.5	1.93	377	149.1	>300	Yes	27.9
PMTP	3.4	1.33	334		84.8	Yes	27.2
PNVTP	7.4	1.96	380	130.2	147.8	Yes	11.6
PSTP	36.1	1.76	381	131.1	153.1	Yes	15.1
POTP	4.67	1.66	337		70.0	Yes	25.7

^a Determined by GPC in THF using PS standard.

^b The temperatures at 5% weight loss of the samples under nitrogen [$T_d(N_2)$] were measured by TGA heating experiments at a rate of 20 °C/min.

^c The glass transition temperatures (T_g) and the melting temperatures (T_m) were obtained from DSC during the second heating process at a rate of 10 °C min $^{-1}$ under nitrogen atmosphere.

^d The transition temperature from LC phase to isotropic phase (T_i) as measured by POM at a heating rate of 10 °C min $^{-1}$ when the inflection light intensity reduced to 50%.

^e The liquid crystallinity was determined by POM.

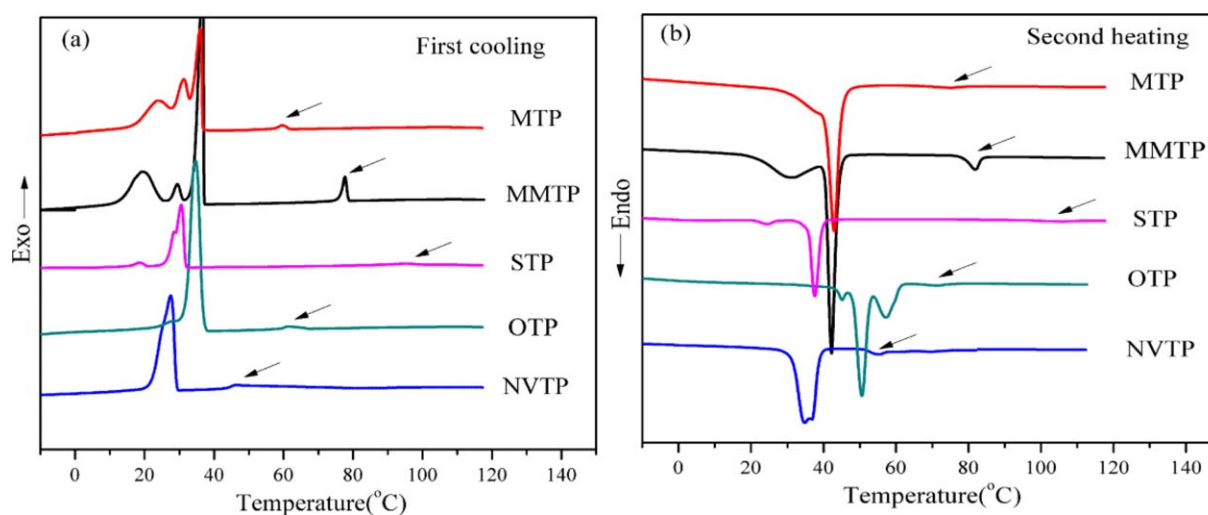


FIGURE 2 DSC curves of MTP, MMTP, STP, SOTP, and NVTP in the first cooling (a) and second heating (b) runs at the rate of 10 °C min $^{-1}$. [Color figure can be viewed at wileyonlinelibrary.com]

Small-angle X-ray scattering (SAXS) experiments were performed with a high-flux SAXS instrument (SAXSess, Anton Paar), equipped with Kratky block-collimation system and a Philips PW 3830 sealed-tube X-ray generator (Cu K α). The wavelength was 0.1542 nm. A highly sensitive SAXS imaging

plate, which was 264.5 mm away from the sample was used to collect the signal in vacuum. Samples were placed in between aluminum foils, which were folded and sandwiched in a steel sample holder. After background subtraction, deconvolution was performed according to the Lake's method.

TABLE 2 Liquid-Crystallinities of the Monomers

Monomer	Phase Transition Temperature (°C)	
	Second Heating	First Cooling
MTP	C 43.1 Φ 74.3 I	C ₁ 24.0 C ₂ 31.5 C ₃ 36.7 Φ 60.4 I
MMTP	C ₁ 30.5 C ₂ 42.1 Φ 82.3 I	C ₁ 19.3 C ₂ 29.4 C ₃ 37.4 Φ 78.3 I
STP	C ₁ 24.5 C ₂ 37.5 Φ 104.6 I	C 30.8 Φ 97.6 I
OTP	C ₁ 50.7 C ₂ 57.4 Φ 71.3 I	C 34.9 Φ 63.7 I
NVTP	C 34.7 Φ 55.9 I	C 26.8 Φ 49.5 I

C, crystal; Φ , columnar phase; I, isotropic state.

RESULTS AND DISCUSSION

Synthesis and Characterization of Monomers and Polymers

A series of Tp-based monomers (MTP, MMTP, STP, SOTP, and NVTP) were successfully synthesized according to the synthetic route, illustrated in Scheme 2. The chemical structures of the monomers were confirmed by ^1H NMR and high-resolution mass spectrometry. Figure 1 shows the ^1H NMR spectra (in CDCl_3 solvent) of the monomers MTP, MMTP, STP, SOTP, and NVTP, respectively. The chemical shifts and peak integrations of all the protons in the monomers are in excellent agreement with their expected structures. The MTP, MMTP, OTP, and STP monomers could be easily polymerized

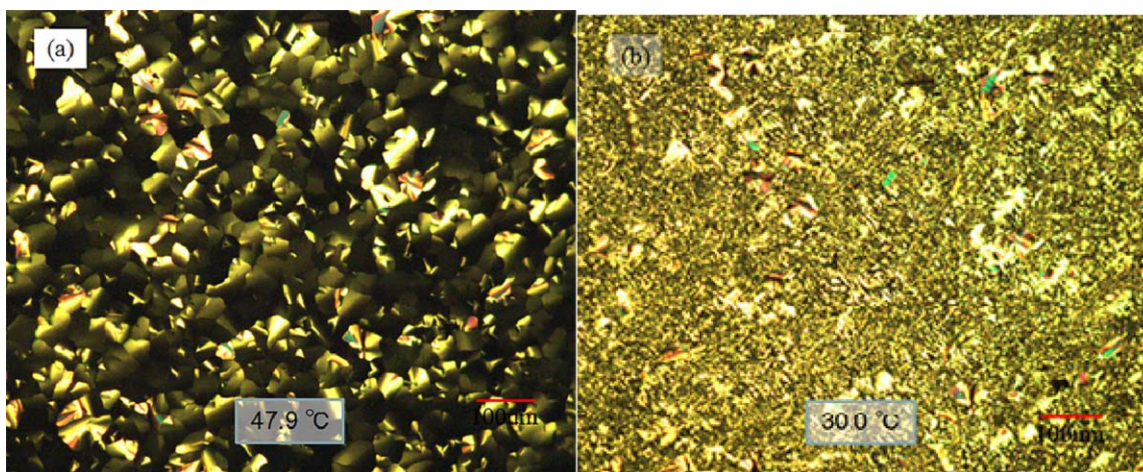


FIGURE 3 Columnar phase texture of MMTP at 47.9 °C (a) and crystal texture of MMTP at 30.0 °C (b). [Color figure can be viewed at wileyonlinelibrary.com]

by free radical polymerization. The PNVTP could be obtained by ROMP. Herein, STP was used as an example for elucidating the process. Figure 1(e,f) shows the ^1H NMR spectra (CDCl_3) of the monomer STP and its polymer PSTP. The characteristic resonances of the vinyl group at 5.41 and 5.92 ppm could be easily seen for the monomer STP in Figure 1(e). After polymerization, characteristic resonances of the vinyl group disappeared completely and the chemical shifts of PSTP were quite broadened in Figure 1(f), which was consistent with the expected polymeric structure. The M_n values of polymers were determined by GPC. The data are summarized in Table 1. The M_n values of these polymers ranged from 3.7×10^4 to $49.5 \times 10^4 \text{ g mol}^{-1}$ with polydispersity indexes of 1.23–1.96, eliminating the influence of M_n on the LC behaviors of the polymers.

Mesomorphic Properties of the Monomers

The thermal behavior of the monomers was studied by a combining DSC and POM techniques. Figure 2(a,b) shows the

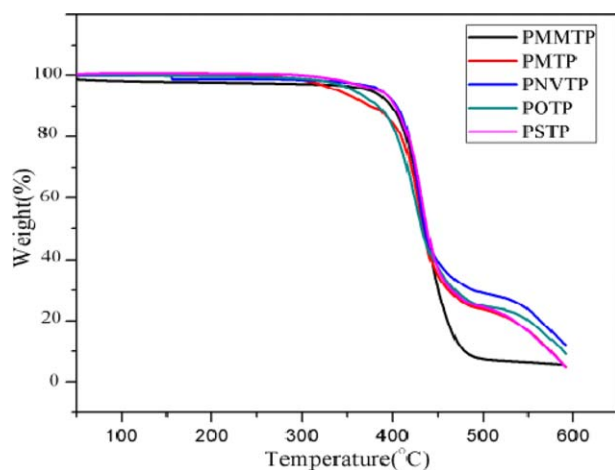


FIGURE 4 TGA curves of polymeric samples in N_2 at a heating rate of 20 °C min^{-1} . [Color figure can be viewed at wileyonlinelibrary.com]

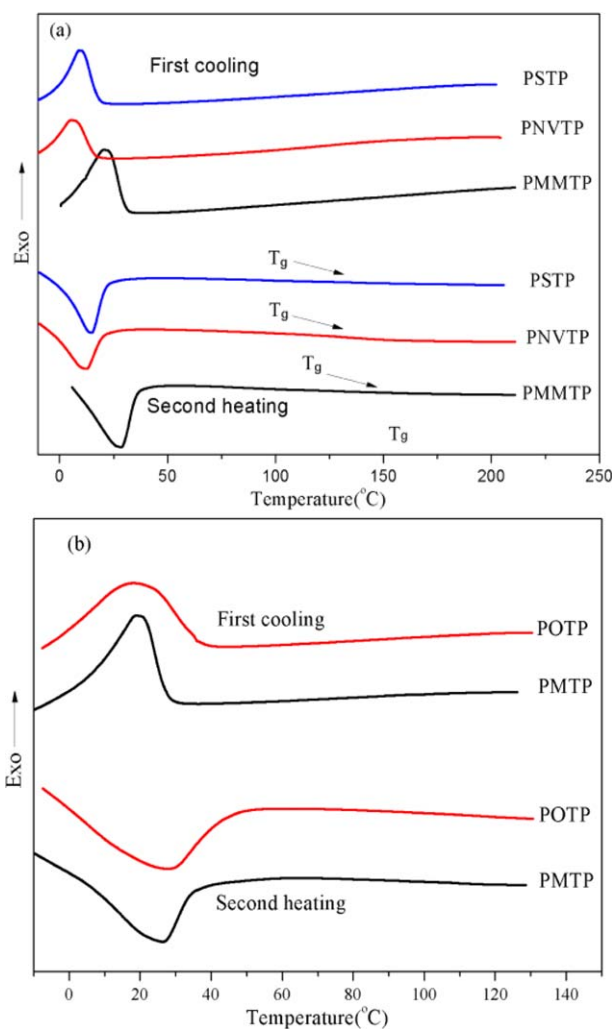


FIGURE 5 DSC curves of (a) PMMTP, PNVTP, and PSTP (b) POTP and PMTP in the first cooling and second heating at the rate of 10 °C min^{-1} . [Color figure can be viewed at wileyonlinelibrary.com]

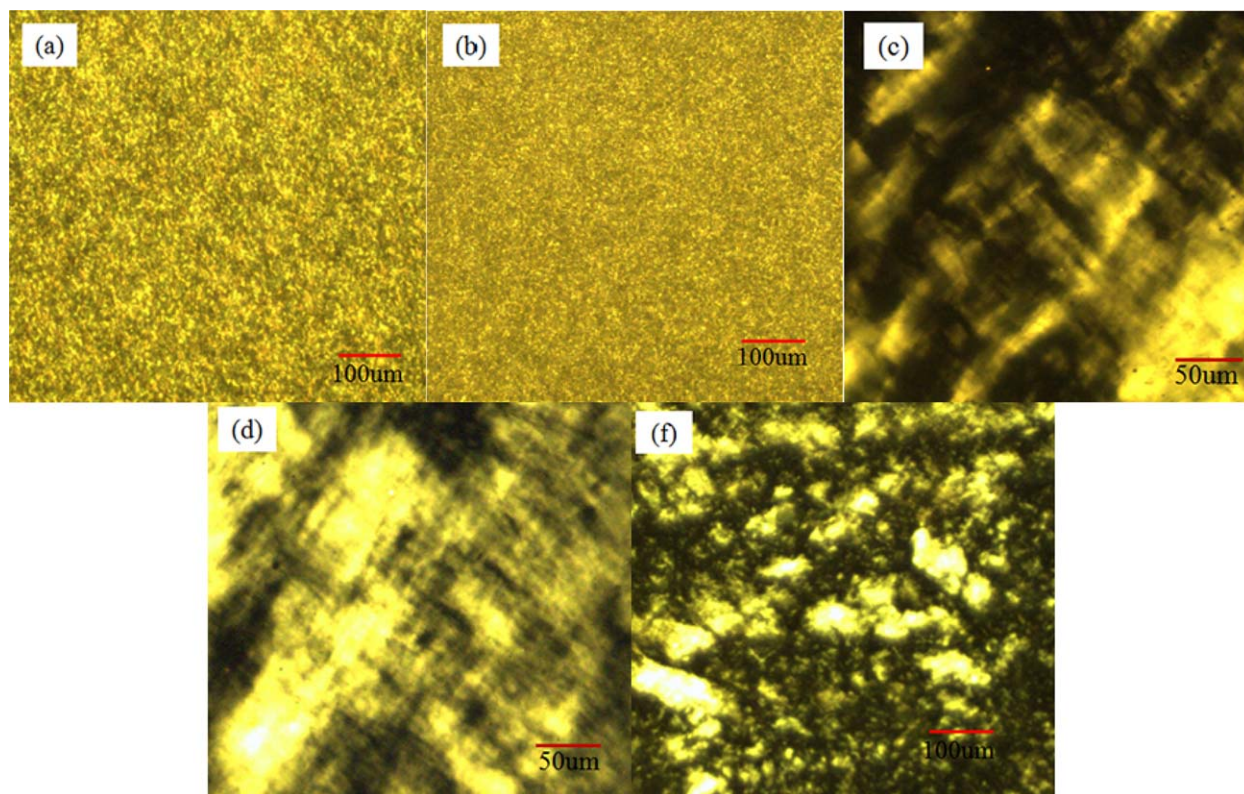


FIGURE 6 Textures of polymers (a) PMTP at 75.3 °C, (b) POTP at 63.7 °C, (c) PNVTP at 140.4 °C, (d) PSTP at 143.6 °C, and (f) PMMTP at 300 °C. [Color figure can be viewed at wileyonlinelibrary.com]

first cooling and the second heating DSC curves of MTP, MMTP, STP, SOTP, and NVTP at a rate of 10 °C min⁻¹, under nitrogen atmosphere after eliminating the thermal history. Table 2 lists the transition temperatures. During the process of cooling or heating, a small exothermic or endothermic peak (marked by an arrow) in the high-temperature region was detected for each monomer. Meantime, the typical

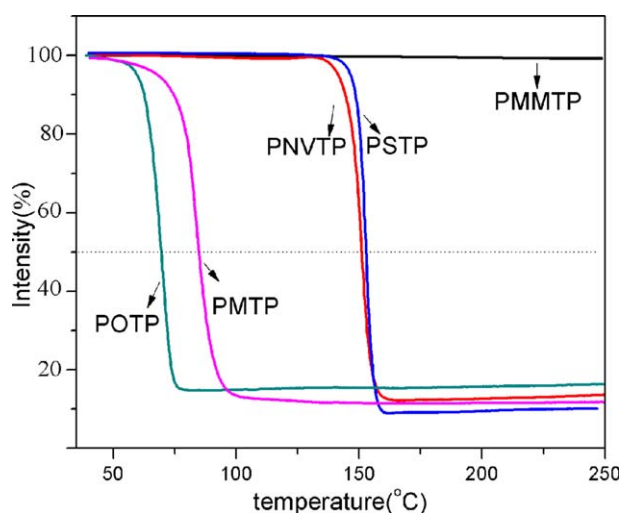


FIGURE 7 The changes in reflection of light intensities for polymers at a heating rate of 10 °C min⁻¹. [Color figure can be viewed at wileyonlinelibrary.com]

pseudo focal-conic texture was observed upon cooling from the isotropic melt [Fig. 3(a)]. This indicated that the formation of the columnar phase was caused by the π - π stacking of the planar TP cores. Therefore, these transition peaks corresponded to the interconversions between isotropic and columnar phases, which indicated the formation of the enantiotropic LC phase. In the low temperature region, a big peak or several small peaks appeared. Combined with the POM results [Fig. 3 (b)], these peaks corresponded to the crystalline melting. In general, the monomers could form the crystalline phase in the low-temperature region and columnar phase in the high-temperature region.

Phase Transitions and Phase Structures of the Polymers

The TGA results of the polymers are shown in Figure 4 and all samples had good thermal stability. The temperatures at 5% weight loss of the samples were above 330 °C under nitrogen at a rate of 20 °C min⁻¹ and details of the decomposition temperatures are shown in Table 1. The thermal and liquid-crystalline properties of the polymers were investigated by a combination of DSC and POM techniques. From the DSC curves (Fig. 5), all polymers showed the melting peaks of long alkane tails on heating and the results are presented in Table 1. For PMMTP, PSTP, and PNVTP, the glass transition was observed.

However, no other peaks were observed in case of all polymers. This phenomenon was often observed for MJLCs. This

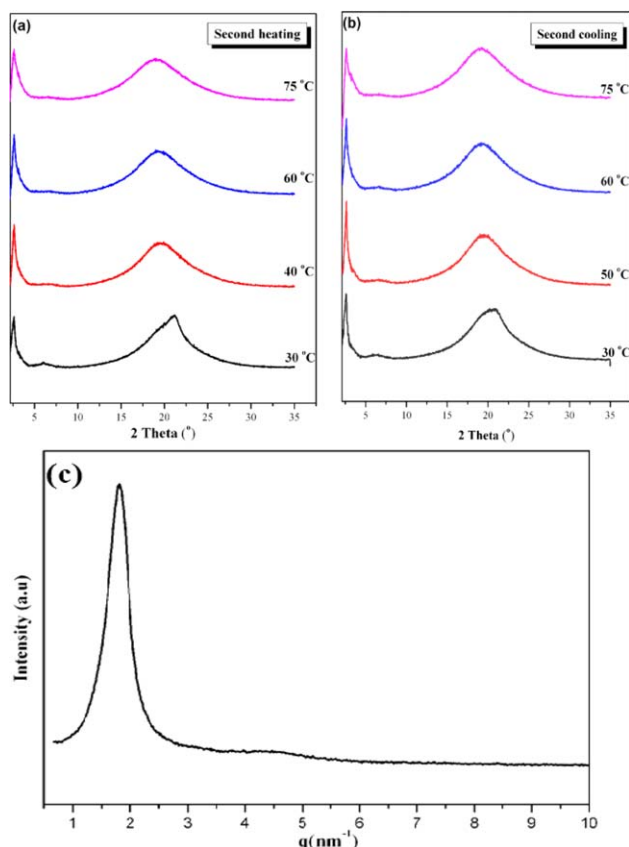


FIGURE 8 1D WAXD patterns of PMTP during the second heating (a) and subsequent cooling (b) and the SAXS profile of PMTP(c). [Color figure can be viewed at wileyonlinelibrary.com]

implied that these polymers had phase structures similar to MJLCs, which was the result of the bulky triphenylene mesogens wrapped around the main chain.

Birefringence of the polymers was studied by POM. For maintaining consistency with DSC analysis, all the samples were heated to 200 °C and then slowly cooled to room temperature. When the temperature was again raised in the second heating scan, the polymers behaved differently depending on the main

chain. Based on this result, the polymers could be divided into three types. First, the PMTP and POTP had a colorful texture at room temperature and also relatively low T_i compared to others polymers. After they were cooled slowly from T_i , the birefringence appeared easily again [Fig. 6(a,b)]. For PSTP and PNVT, no birefringence was observed in the heating process, until they were annealed for a long time below the T_i [Fig. 6(c,d)]. Lastly, when PMMTP [Fig. 6(f)] was heated to 300 °C, the sample showed a colorful texture throughout the process. From the POM results, it was evident that all polymers could form the LC phase.

To get more insight into the phase transition temperature, reflection light intensity (birefringence) measurements were carried out. This was due to the fact that it was difficult to detect the phase transition temperatures of samples by DSC. The curves for changes in reflection of light intensity are shown in Figure 7. For maintaining consistency with DSC analysis, all samples were heated uniformly at the rate of 10 °C min⁻¹. From the figure, it was evident that the polymers showed obvious transitions at their respective clearing temperatures (T_i) (reflection of light intensity was observed at 50%), which indicated a transition from the ordered state to isotropic state. The results are presented in Table 1. Although the polymers contained the same side chains, the T_i values of polymers were different.

Phase Structure Identification of the Polymer

To get more information on molecular arrangements of the polymers, temperature dependent 1D WAXD, 2D WAXD, and SAXS experiments were performed. For the 1D WAXD experiment, about 60 mg of each polymer was taken in an aluminum foil substrate. The samples were then heated to their T_i temperatures (PMTP was heated to 280 °C) and then annealed for 10 h below the T_i temperature. From the 1D WAXD experimental results, no obvious diffractions were observed in $2\theta \approx 25^\circ$ for all polymers, which represented π - π stacking in a discotic LC columnar layout. This suggested that the Tp mesogens could not self-organize as well-ordered supramolecular columns, due to the strong coupling effects between the main chain and Tp. However, at low angles, the

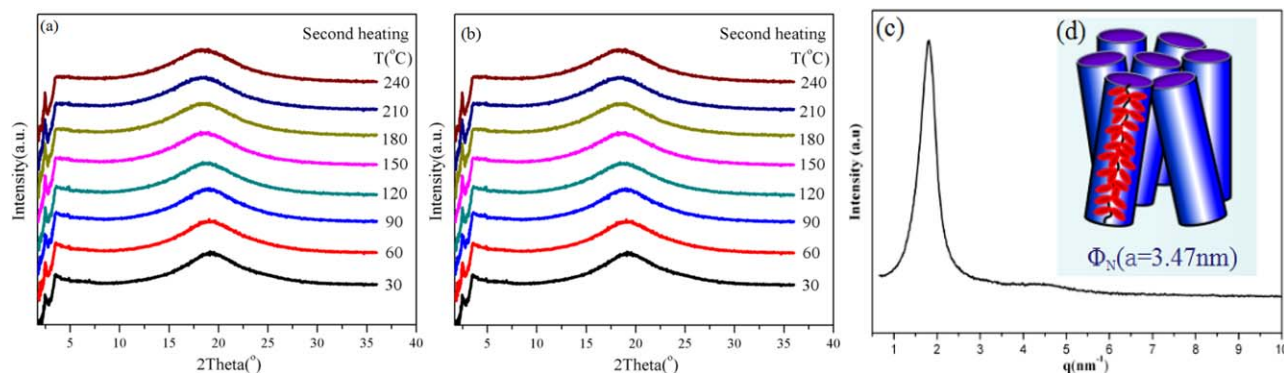


FIGURE 9 1D WAXD patterns of PMMTP during the second heating (a) and subsequent cooling (b), the SAXS profile of PMMTP (c), and the schematic representation of the molecular packing of PMMTP and PMTP (d). [Color figure can be viewed at wileyonlinelibrary.com]

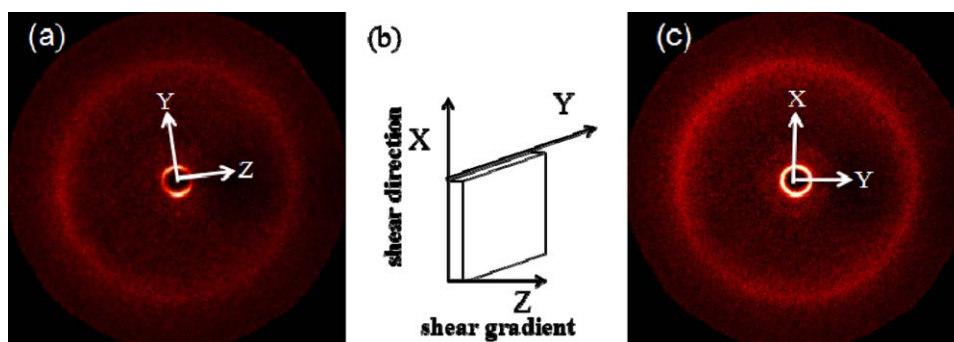


FIGURE 10 2D WAXD patterns of PMMTP at room temperature, with the X-ray beam perpendicular (a) and parallel (c) to the shear direction, (b) shearing geometry. [Color figure can be viewed at wileyonlinelibrary.com]

samples showed different diffraction peaks, which implied that the polymers formed structures with different phases. From the XRD results, the polymers could be divided into three categories based on phase structures.

PMTP and PMMTP belonged to the first kind. Figure 8(a,b) illustrates the temperature-variable 1D WAXD patterns of PMTP from 30 to 75 °C and from 75 to 30 °C during the second heating and subsequent cooling runs. And the range of 2θ was from 1.5° to 35°.

A strong reflection peak at low angle was observed at $2\theta = 2.55^\circ$ ($d = 3.47$ nm), and there was no other narrow reflection peak at the low angle. After the sample was heated to 75 °C, the reflection peak appeared as a broad halo. At a high angle, a slightly sharp diffraction peak at $2\theta = 20^\circ$ (d spacing of 0.44 nm) appeared, which was the result of a crystalline long-alkyl tail at low temperature. The SAXS results Figure 8(c) further confirmed the phase structure of PMTP. From the diffraction pattern, only one diffraction peak was observed at a low angle with

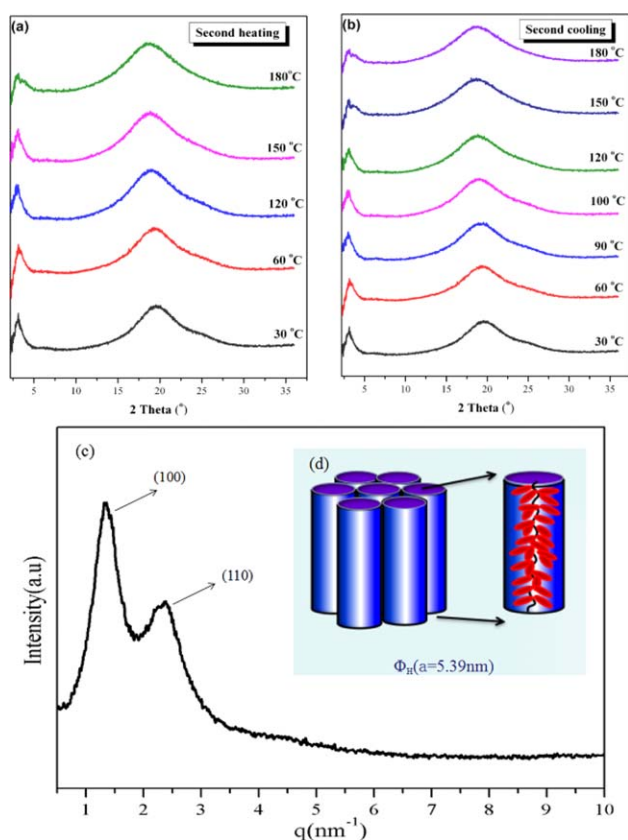


FIGURE 11 1D WAXD patterns of PNVT during the second heating (a) and subsequent cooling (b), SAXS profile of PNVT, and (c) the schematic representation of the molecular packing of PNVT (d). [Color figure can be viewed at wileyonlinelibrary.com]

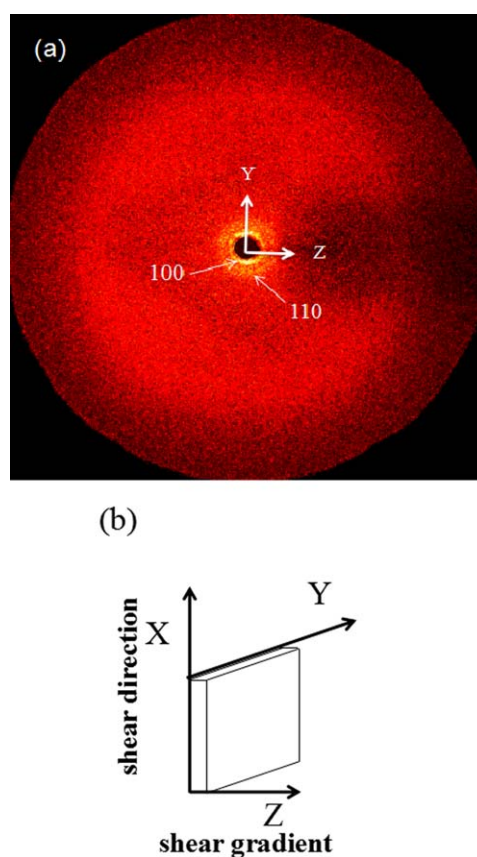


FIGURE 12 2D WAXD patterns of PNVT at room temperature with X-ray beam perpendicular to (a) shear direction, shearing geometry (b). [Color figure can be viewed at wileyonlinelibrary.com]

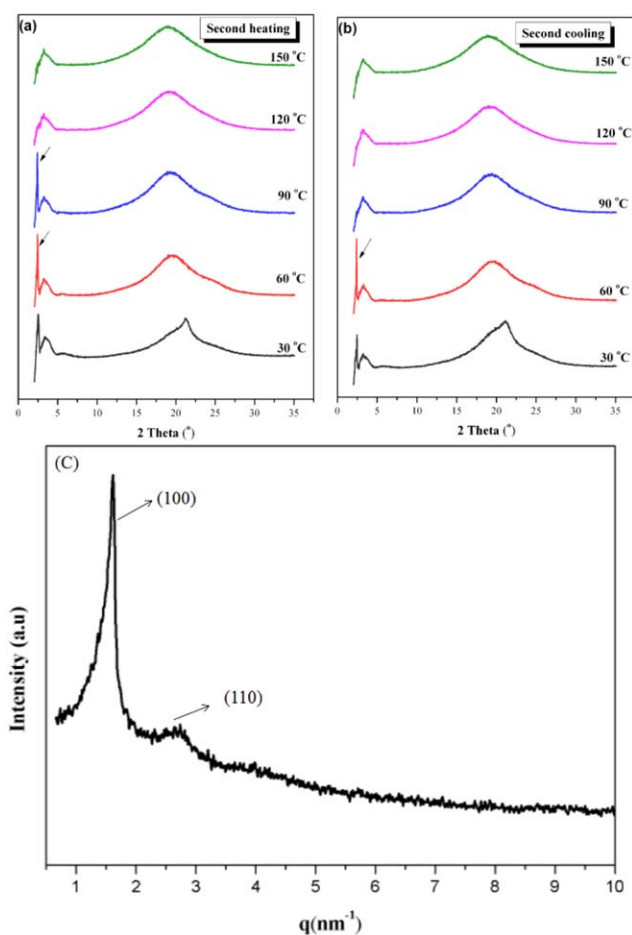


FIGURE 13 1D WAXD patterns of the POTP during the second heating (a) and subsequent cooling (b), SAXS profile of POTP (c). [Color figure can be viewed at wileyonlinelibrary.com]

$q = 1.81 \text{ nm}^{-1}$ and the corresponding d -spacing of 3.47 nm, which was consistent with the 1D WAXD. The 1D WAXD and SAXS results of PMMTP (Fig. 9) were extremely similar to that of PMTP. As seen in Figure 9(a,b), in case of either heating or cooling, a strong diffraction peak appeared in the whole process, which indicated that the polymer exhibited the LC phase. This was also consistent with the POM results. To further confirm the phase structure of PMMTP, 2D WAXD experiments were performed. The oriented sample was prepared by mechanically shearing a film with a thickness of $\approx 1 \text{ mm}$ at 245 °C and then annealing at 80 °C overnight. Figure 10(a) shows the 2D WAXD profiles of PMMTP, with X-ray beam perpendicular to the direction of the shear. A pair of diffraction arcs was observed at a low-angle, which indicated that an ordered structure was formed at the nanometer level. When the X-ray beam was parallel to the direction of shear [Fig. 10(c)], a ring pattern at $2\theta = 2.55^\circ$ (d -spacing = 3.47 nm) was observed, which indicated that the intensity distribution was isotropic. Considering the similarity of the X-ray results to the previously reported results, it may be proposed that PMMTP and PMTP exhibited a columnar nematic (Φ_N) phase, in which each cylinder could be attributed to a single polymeric chain with the side groups tightly jacketing the backbone. Moreover, it was interesting to find that

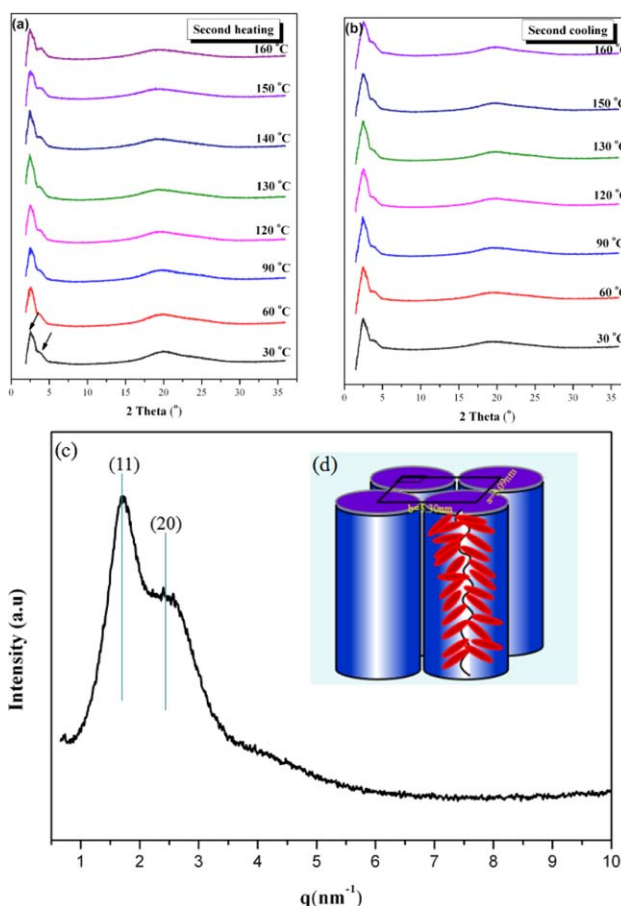


FIGURE 14 1D WAXD patterns of PSTP during the second heating (a) and subsequent cooling (b), SAXS profile of PSTP (c), and the schematic drawing of the molecular packing of PSTP (d). [Color figure can be viewed at wileyonlinelibrary.com]

the column diameters of PMTP and PMMTP were the same (3.47 nm) [Fig. 9(d)].

PNVTP and POTP belonged to the second category. Figure 11(a,b) shows the temperature-variable 1D WAXD patterns of PNVTP from 30 to 180 °C and from 180 to 30 °C in the 2θ range of 2.5° to 30°. Only one peak at $2\theta = 3.29^\circ$ was observed at the low-angle. On heating to 150 °C, the peak

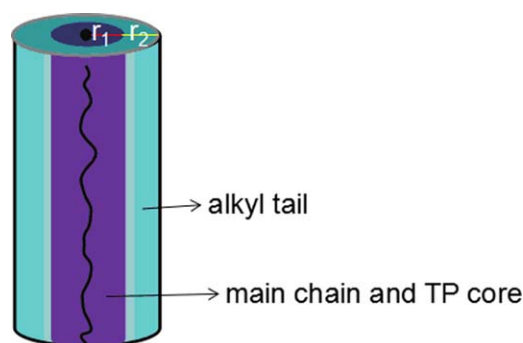


FIGURE 15 The structural representation of the cylinder. [Color figure can be viewed at wileyonlinelibrary.com]

TABLE 3 The Diameter of the Column, the Length of Rigid Moieties of Side Chain, the Length of Long Alkyl Tail Stretching, and Deduced Angle Between TP Mesogen and Main Chain

Sample	LC phase	d^a (nm)	r_1^b (nm)	r_2^c (nm)	r^d (nm)	Angle ^e (°)
PMTP	Φ_N	3.47	0.98	2.02	3.00	35
PMMTP	Φ_N	3.47	0.98	2.02	3.00	35
PNVTP	Φ_H	5.39	1.92	2.02	3.94	43
POTP	Φ_H	4.55	1.59	2.02	3.61	39
PSTP	Φ_R	/	1.61	2.02	3.63	/

^a Experimentally determined diameter of the column of Φ_N and diameter between the two columns of Φ_H .

^b The length of rigid moieties of side chain.

^c The length of long alkyl tail stretching as all-trans conformation.

^d The ideal length of side chain.

^e Deduced angle between TP mesogen and main chain.

became diffuse, which implied that the orderliness in the structure had been destroyed. Upon cooling, the diffraction peak reappeared, which indicated the formation of an ordered structure. The sample was further studied by SAXS, the results of which are shown in Figure 11(c). Compared to the 1D WAXD results, a sharp first-order peak centered at $q_1 = 1.35 \text{ nm}^{-1}$ and a second-order diffraction peak appeared at $q_2 = 2.34 \text{ nm}^{-1}$. The ratio of the scattering vectors of the two peaks $q_1: q_2$ was 1: $3^{1/2}$, which suggested a hexagonal columnar (Φ_H) phase. The corresponding d -spacings were 4.65 nm and 2.67 nm, which could be assigned as (100) and (110) diffractions of the hexagonal structure with $a = 5.39$ nm. Therefore, the peak appeared at low angle in the 1D WAXD pattern is the second diffraction peak and the missed first-order diffraction cannot be detected own to exceed the test range. Figure 12(a) shows 2D WAXD of PNVTP with the X-ray beam perpendicular to the direction of shear. Two pairs of diffraction arcs attributed to (100) and (110) diffractions were located on the meridian. The result confirmed the hexagonal packing of cylinders. Due to the steric effect of side chain and the strong coupling effect between the main chain and TP mesogens, the TP-based mesogens could not form ordered structures. This resulted in the disappearance of d -spacing of 0.36 nm, which was unique feature of π - π stacking in the discotic LC columns. The schematic representation of the molecular packing of PNVTP is shown in Figure 11(d).

Figure 13 shows temperature dependent 1D WAXD and SAXS of POTP. Diffraction in the low region at 2.41 was detected. The peak that appeared at 2.41 in Figure 13(a), disappeared at high temperature, which indicated that the orderly structure was destroyed. On cooling, the ordered structure was formed again [Fig. 13(b)]. In the high 2θ range of 10–35°, at lower temperature, the WAXD patterns showed only one peak, which showed the typical crystal formed by the long alkoxy tails. In the SAXS results [Fig. 13(c)], two peaks also were observed with q -values of 1.61 and 2.75 nm^{-1} at the low-angle and the ratio of the scattering

vectors of the two peaks $q_1: q_2$ was 1: $3^{1/2}$. Hence, both POTP and PNVTP showed the Φ_H phase.

PSTP belonged to the third category. When an ether bond (POTP) was replaced by an ester bond (PSTP), PSTP showed a different phase structure. Results of temperature dependent 1D WAXD experiment of PSTP are shown in Figure 14(a,b). Two peaks were visible at the low-angle, which were close to each other when heating or cooling. The scattering vector ratio of the diffractions was 1: $2^{1/2}$. These two peaks also appeared in SAXS [Fig. 14(c)] and the corresponding q values were 2.47 and 1.71 nm^{-1} , respectively. It could be speculated that the PSTP formed a rectangular columnar (Φ_R) phase and the two peaks at the low angle could be assigned as (11) and (20) with $a = 5.09$ nm and $b = 5.30$ nm [Fig. 14(d)].

Phase Predictions

To get a clear idea of the columnar phases formed by the backbone and TP moieties, the model showing the packing of the columns is shown in Figure 15. The columns were comprised of two parts: the core and shell. The core (the central portion of column) included the main chain and TP core (r_1) and the shell included the alkyl tail (r_2). The radius of the central portion of column changed as the backbone changed, but the thickness of outer layer remained the same. As shown in Table 3, compared to the diameters of columns from the SAXS results, the ideal lengths of side chains were much larger. As for this, it was considered that the cylinders of the polymers were similar to the cylinders of MJLCPs, which were formed by the “jacketing effect” of rod-like supramolecular mesogens. It meant that the TP mesogens were tilted away from the main chains. From simulation, the length of the alkyl tail with all-trans was about 2.02 nm. For PMTP and PMMTP, the diameter of column was 3.47 nm. This suggested that the TP mesogen tilted to an angle of $\sim 35^\circ$ off the main chain. For PNVTP and POTP, the triphenylene side chain wrapped itself around the main chains to form columnar-shaped molecules with diameters of 5.39 and 4.55 nm, respectively. The corresponding tilt angle was 43° and 39° , respectively.

CONCLUSIONS

In summary, a series of SCLCPs with different main chains, containing TP mesogenic groups with the same long-alkyl tails (PMTP, PMMTP, PSTP, POTP, and PNVTP) were successfully synthesized. Although the monomers had bulky mesogenic pendants, all polymers were easily obtained by conventional solution radical polymerization or ring-open metathesis polymerization. The M_n of the polymers were in the range of 3.4×10^4 to $49.5 \times 10^4 \text{ g}\cdot\text{mol}^{-1}$. All the polymers were thermally stable. The phase structures and transitions of the polymers were investigated by DSC, POM, and WAXD. The results showed that all the polymers exhibited properties typical of MJLCPs. In other words, irrespective of the structure of main chain, all the polymers presented the columnar phase, in which the TP mesogens were wrapped around the main chains. However, the phase transition temperature strongly depended on the main chain. This work

provided a new perspective to understand the structure–property relationships of SCLCPs.

ACKNOWLEDGMENTS

This research was financially supported by the National Nature Science Foundation of China (21504075) and the Research Foundation of Education College of Hunan Province, China (Grant No. 14C1090).

REFERENCES AND NOTES

- S. Hassan, R. Anandakathir, M. J. Sobkowicz, B. M. Budhlall, *Polym. Chem.* **2016**, *7*, 1452–1460.
- O. T. Picot, M. Dai, D. J. Broer, T. Peijs, C. W. Bastiaansen, *ACS Appl. Mater. Interfaces* **2013**, *5*, 7117–7121.
- Z. Q. Yu, T. T. Li, Z. Zhang, J. H. Liu, W. Z. Yuan, J. W. Y. Lam, S. Yang, E. Q. Chen, B. Z. Tang, *Macromolecules* **2015**, *48*, 2886–2893.
- N. Gimeno, I. Pintre, M. Martínez-Abadía, J. L. Serrano, M. B. Ros, *RSC Adv.* **2014**, *4*, 19694.
- S. Chen, A. Ling, H. L. Zhang, *J. Polym. Sci. Part A: Polym. Chem.* **2013**, *51*, 2759–2768.
- P. Kohn, L. Ghazaryan, G. Gupta, M. Sommer, A. Wicklein, M. Thelakkat, T. Thurn-Albrecht, *Macromolecules* **2012**, *45*, 5676–5683.
- L. Angiolini, T. Benelli, L. Giorgini, *React. Funct. Polym.* **2011**, *71*, 204–209.
- M. Kamachi, X. S. Cheng, T. Kida, A. Kajiwara, M. Shibasaka, S. Nagata, *Macromolecules* **1987**, *20*, 2665–2669.
- C. Y. Ba, Z. R. Shen, H. W. Gu, G. Q. Guo, P. Xie, R. B. Zhang, C. F. Zhu, L. J. Wan, F. Y. Li, C. H. Huang, *Liq. Cryst.* **2003**, *30*, 391–397.
- M. Kamachi, *Macromol. Symp.* **1998**, pp 69–79.
- A. Bacher, I. Bleyl, C. H. Erdelen, D. Haarer, W. Paulus, H. W. Schmidt, *Adv. Mat.* **1997**, *9*, 1031–1035.
- B. Mu, B. Wu, S. Pan, J. Fang, D. Chen, *Macromolecules* **2015**, *48*, 2388–2398.
- B. Mu, S. Pan, H. Bian, B. Wu, J. Fang, D. Chen, *Macromolecules* **2015**, *48*, 6768–6780.
- W. Kreuder, H. Ringsdorf, *Rapid Commun.* **1983**, *4*, 807–815.
- B. Wu, B. Mu, S. Wang, J. Duan, J. Fang, R. Cheng, D. Chen, *Macromolecules* **2013**, *46*, 2916–2929.
- S. Q. Yang, W. Qu, H. B. Pan, Y. D. Zhang, S. J. Zheng, X. H. Fan, Z. Shen, *Polymer* **2016**, *84*, 355–364.
- T. Makowski, T. Ganicz, W. Zajaczkowski, W. Pisula, W. Stanczyk, A. Tracz, *Express Polym. Lett.* **2015**, *9*, 636–646.
- O. A. Otmakhova, S. A. Kuptsov, R. V. Talroze, T. E. Patten, *Macromolecules* **2003**, *36*, 3432–3435.
- I. Tahar-Djebbar, F. Nekelson, B. Heinrich, B. Donnio, D. Guillon, D. Kreher, F. Mathevet, A. Attias, *J. Chem. Mater.* **2011**, *23*, 4653–4656.
- B. Hüser, T. Pakula, H. Spiess, *Macromolecules* **1989**, *22*, 1960–1963.
- S. Disch, H. Finkelmann, H. Ringsdorf, P. Schuhmacher, *Macromolecules* **1995**, *28*, 2424–2428.
- C. T. Imrie, R. T. Inkster, Z. Lu, M. D. Ingram, *Mol. Cryst. Liq. Cryst.* **2004**, *408*, 33–43.
- I. Bleyl, C. Erdelen, K. H. Etzbach, W. Paulus, H. W. Schmidt, K. Siemensmeyer, D. Haarer, *Mol. Cryst. Liq. Cryst. Sci. Technol. Sect. A* **1997**, *299*, 149–155.
- D. Zeng, I. Tahar-Djebbar, Y. Xiao, F. Kameche, N. Kayunkid, M. Brinkmann, D. Guillon, B. Heinrich, B. Donnio, D. A. Ivanov, E. Lacaze, D. Kreher, F. Mathevet, A. Attias, *J. Macromol.* **2014**, *47*, 1715–1731.
- C. Xing, J. W. Lam, K. Zhao, B. Z. Tang, *J. Polym. Sci. Part A: Polym. Chem.* **2008**, *46*, 2960–2974.
- Z. Q. Yu, J. W. Y. Lam, K. Zhao, C. Z. Zhu, S. Yang, J. S. Lin, B. S. Li, J. H. Liu, E. Q. Chen, B. Z. Tang, *Polym. Chem.* **2013**, *4*, 996–1005.
- Y. F. Zhu, H. J. Tian, H. W. Wu, D. Z. Hao, Y. Zhou, Z. Shen, D. C. Zou, P. C. Sun, X. H. Fan, Q. F. Zhou, *J. Polym. Sci. Part A: Polym. Chem.* **2014**, *52*, 295–304.
- Y. F. Zhu, X. L. Guan, Z. Shen, X. H. Fan, Q. F. Zhou, *Macromolecules* **2012**, *45*, 3346–3355.
- J. Ban, S. Chen, H. Zhang, *RSC Adv.* **2014**, *4*, 54158–54167.
- J. Ban, *Chin. J. Polym. Sci.* **2015**, *33*, 1245–1259.
- W. Qu, X. Zhu, J. Chen, L. Niu, D. Liang, X. Fan, Z. Shen, Q. Zhou, *Macromolecules* **2014**, *47*, 2727–2735.
- G. Jiang, H. Cai, Z. Shen, X. Fan, Q. Zhou, *J. Polym. Sci. Part A: Polym. Chem.* **2013**, *51*, 557–564.
- S. Chen, J. Qiu, H. L. Xie, H. L. Zhang, *J. Polym. Sci. Part A: Polym. Chem.* **2013**, *51*, 2804–2816.
- X. Mei, J. Zhang, Z. Shen, X. Wan, *Polym. Chem.* **2012**, *3*, 2857.
- H. Wu, L. Zhang, Y. Xu, Z. Ma, Z. Shen, X. Fan, Q. Zhou, *J. Polym. Sci. Part A: Polym. Chem.* **2012**, *50*, 1792–1800.
- S. Chen, C. Jie, H. Xie, H. Zhang, *J. Polym. Sci. Part A: Polym. Chem.* **2012**, *50*, 3923–3935.
- Q. K. Zhang, H. J. Tian, C. F. Li, Y. F. Zhu, Y. Liang, Z. Shen, X. H. Fan, *Polym. Chem.* **2014**, *5*, 4526.
- H. Jin, Y. Xu, Z. Shen, D. Zou, D. Wang, W. Zhang, X. Fan, Q. Zhou, *Macromolecules* **2010**, *43*, 8468–8478.
- J. F. Zheng, Z. Q. Yu, X. Liu, X. F. Chen, S. Yang, E. Q. Chen, *J. Polym. Sci. Part A: Polym. Chem.* **2012**, *50*, 5023–5031.
- Q. Tan, J. Liao, S. Chen, Y. Zhu, H. Zhang, *Polym. Chem.* **2014**, *5*, 5147.
- Y. F. Zhu, Z. Y. Zhang, Q. K. Zhang, P. P. Hou, D. Z. Hao, Y. Y. Qiao, Z. Shen, X. H. Fan, Q. F. Zhou, *Macromolecules* **2014**, *47*, 2803–2810.